An Opening Profile Recognition Method for MFL Signals of Defect

Songling Huang[1], *Senior Member, IEEE*, Lisha Peng[1], *Student Member, IEEE*, Qing Wang[2], *Senior Member, IEEE*, Shen Wang[1], and Wei Zhao[1]

***Abstract*—The defect opening profile recognition is of great concern in the magnetic flux leakage (MFL) measurement technique. The detected spatial MFL signal has three components: horizontal, vertical and normal component. Horizontal and normal component signals are commonly used to estimate the defect profile, while the vertical component has always been neglected. With the development of the high resolution and the three-dimension MFL testing techniques, the vertical component signal is become more available. This paper analyzes the essential right-angle features of the vertical component signal, which is useful for the defect opening profile recognition. After obtaining the initial profile form the horizontal or normal component and identifying the types of right-angle from the vertical component, the opening profile is further optimized based on these right-angle features. The opening profile recognition method is put forward in this paper to improve the accuracy of the recognition result. Both simulation and experimental tests are conducted to verify the well performance of the proposed method. Compared with the opening profiles recognized merely by horizontal component signal, the proposed method shows better recognition results, which also validates that the vertical component signal can also be a useful information for the defect estimation.**

***Index Terms*—Magnetic flux leakage (MFL) signal, vertical component, right-angle feature, opening profile recognition**

I. Introduction

MAGNETIC flux leakage (MFL) testing is an effective nondestructive testing (NDT) technique, which is widely used to analyze the defect in ferromagnetic material [1-5], e.g. tank floor or oil & gas pipeline, and estimate the profile of defect [6-9]. Under the condition of saturation magnetization, the flawed region in the ferromagnetic material is characterized by a region of high magnetic reluctance causing an increased magnetic leakage field. Thus, the MFL signal of defect can be obtained by the magnetic sensors and used for further analysis. The ability to recognize the shape of defect in the ferromagnetic material from the obtained MFL signals is of critical importance [10]; and the opening profile is a key parameter for describing the shape of defect. Besides, the fortiori accurate defective profile recognition will provide wider application prospects for MFL testing technique.

The spatial MFL signal has three components: horizontal component, vertical component and normal component. Each component of MFL signal carries lots of profile information of the defect [11]. The horizontal component signal, along the direction of magnetization, or the normal component, perpendicular to the material plate, is commonly used to analyze and estimate the defect. This is mainly because of their lager signal strength and better performance on the edge detection of defect. Especially for the traditional one-dimension (1-D) MFL testing, only one component signal is measured. Thus, the horizontal or normal component signal is more prone to be chosen rather than the vertical component signal.

Many researchers have devoted to recognize the profile of defect based on either the horizontal component or normal component of MFL signal. Such as M. Ravan et al. used the horizontal component of the leakage magnetic field to estimate the opening profile of defect with the Canny edge detection algorithm in [12]. R. K. Amineh et al. adopted the normal component signal to shape the surface-breaking cracks in [13]. F. M. Li et al. employed a modified harmony search algorithm to reconstruct the defect profiles in pipelines based on both horizontal and normal component signal in [14]. All these works focused on the horizontal or normal component of MFL signal. The vertical component of MFL signal has less been considered.

However, the vertical component of MFL signal also conveys some useful profile features of defect, which can be fully used for the defect estimation. [15] indicates that the vertical component signal contains the essential right-angle features of defect. This feature is particular for the vertical component signal rather than horizontal or normal component signal. On the other hand, with the development of high resolution or even the extra-high resolution MFL testing technique [16, 17], both the sensitivity and accuracy of the measured signal, obviously including the vertical component signal, have been greatly improved. The latest three-dimension MFL testing technique [18, 19] also provides the possibility for the application of the vertical component signal, comparing with the traditional 1-D MFL testing technique. Thus, besides the commonly used horizontal or normal component signal, combining with the useful information of the vertical component signal to recognize the opening profile of defect can be an available and effective resolution.

Manuscript received July 10, 2018. This work was supported in part by the National Natural Science Foundation of China (NSFC) under Grant No. 51677093 and the National Key Scientific Instrument Development Projects under Grant No 2013YQ140505.

Songling Huang, Lisha Peng, Shen Wang, and Wei Zhao are with the Department of Electrical Engineering, Tsinghua University, Beijing, 100084, China (e-mail: huangsling@tsinghua.edu.cn; pls14@mails.tsinghua.edu.cn; wangshen@mail.tsinghua.edu.cn; zhaowei@mail.tsinghua.edu.cn).

Qing Wang is with the Department of Engineering, Durham University, Durham DH1 3LE, United Kingdom (e-mail: qing.wang@durham.ac.uk).

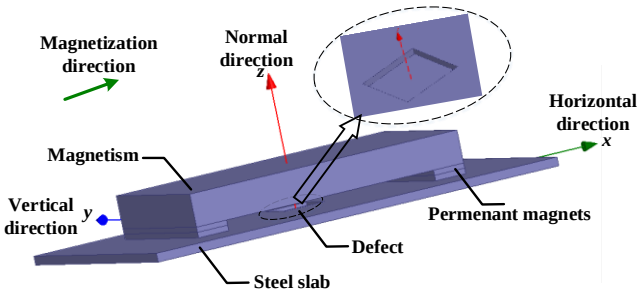

Fig. 1. 3-D finite element simulation model

Based on the characteristic analysis of each component of MFL signal, especially for the right-angle feature of the vertical component signal, this paper proposed an opening profile recognition method of defect. In this method, the initial opening profile is firstly obtained by the horizontal or normal component signal. Then, by the identifying the right-angle features of defect, the opening profile is further optimized by the vertical component signal. This method is suitable for recognizing the opening profile of arbitrary defect and can achieve a more accurate result than that only based on the horizontal or normal component signal. Both the simulation and experimental tests are conducted here to examine the validation of the proposed method, which show the good performance on the opening profile recognition of defect.

The rest of this paper is organized as follows. In Section II, the characteristics of the three components of MFL signal are analyzed, and the right-angle feature of the vertical component signal has been discussed in detail. Section III proposes an identification procedure to distinguish the different features from the vertical component signal and identify the right-angle type of defect. Section IV puts forward an opening profile recognition method of defect with four steps. The feasibility and efficiency of the proposed method is verified in both simulation and experimental tests in Section V. Section VI discusses the conclusion and contribution of this paper.

II. Characteristic Analysis of MFL Signals

The spatial MFL signal contains horizontal, vertical and normal components. Each component signal presents different characteristics of defect response. A three-dimensional (3-D) finite element model is established here to obtain the spatial signals and the characteristics of the three components of MFL signal *Bx*, *By* and *Bz* are analyzed.

A. 3-D Finite Element Model

In the MFL measurement system, the leakage magnetic field distribution for the nonlinear permanent magnetic system follows the basic law of the Maxwell equation [20]. The electromagnetic phenomenon can be expressed as follows.

$$\nabla \times \boldsymbol{H} = \boldsymbol{J} \tag{1}$$

$$\boldsymbol{B} = \mu_0(\boldsymbol{H} + \boldsymbol{M}) \tag{2}$$

$$\boldsymbol{B} = \nabla \times \boldsymbol{A} \tag{3}$$

This lead to

$$\nabla \times \mathbf{A} \times \mathbf{A} = \mu_0(\mathbf{J} + \nabla \times \mathbf{M}) \tag{4}$$

Where $\boldsymbol{B}$, $\boldsymbol{H}$ and $\boldsymbol{M}$ are the magnetic strength, magnetic field strength and magnetization, respectively and μ_0, $\boldsymbol{A}$ and $\boldsymbol{J}$ are the permeability of vacuum, the magnetic vector potential and the current density, separately.

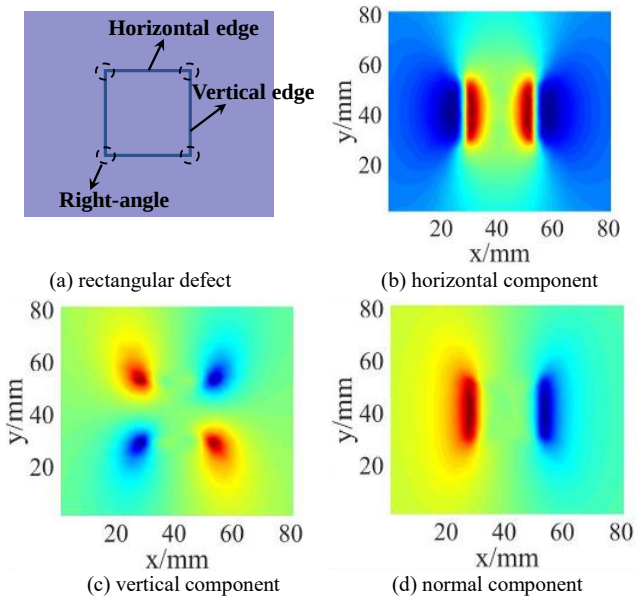

(a) rectangular defect (b) horizontal component

(c) vertical component (d) normal component

Fig. 2. Images of the three component signals of a rectangular defect

The equation (4) can be iteratively solved by finite element numerical method [21] using the Ansoft Maxwell 14.0 software. Fig.1 establishes a finite element model to simulate the 3-D magnetic field of the surface defect in a steel slab. The slab is saturated magnetization by two parallel permanent magnets. The magnetic circuit is closed through the magnetism, permanent magnets and the steel slab. There is a certain lift off distance between the measurement plane and the surface of slab.

The direction of each component of the MFL signal is defined as follows. The direction of the horizontal component *Bx* is parallel to the magnetization direction. The direction of the vertical component *By* is perpendicular to the magnetization direction on the measurement plane. The direction of the normal component *Bz* is perpendicular to the detection plane. In some other literatures, especially for pipeline MFL testing, these three components *Bx*, *By* and *Bz* are also called the axial, circumferential and radial component, separately.

It should be noticed that, the amplitude of the MFL signal simulated by the finite element may not match the absolute values of the real MFL signal obtained by the measurement system, due to the difference of the parameters of the magnetization settings. However, their normalized field distributions match reasonably well. Since the opening profile recognition of defect mainly depends on the magnetic field distributions rather than its amplitude, the MFL signals analyzed here are normalized. Henceforth, when each component of MFL signal is referred in the following context, it implicitly means the normalized signal.

B. Characteristics of Horizontal and Normal MFL Signals

In order to analyze the characteristics of different component signals, Fig.2. gives the pseudo-color images of the normalized three component MFL signals of a rectangular defect. Figs.2. (a) and (b) are the images of horizontal and normal components,

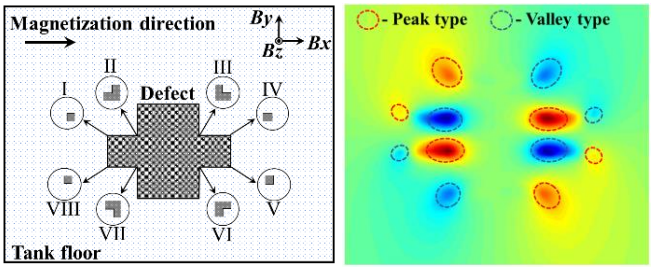

(a) Eight kinds of right angle (b) Vertical component responses

Fig. 3. Eight kinds of right angle and their MFL signal responses.

TABLE I
CLASSIFICATION OF DIFFERENT KINDS OF RIGHT-ANGLE

Type	right angle of defect			
Peak type	I	III	V	VII
Valley type	II	IV	VI	VIII

separately.

The horizontal component signal *Bx* reflects the changing trend of the MFL signal in the horizontal direction. As shown in Fig.2. (a), *Bx* is sensitive to the vertical edges of defect. It has significant fluctuations around the vertical edge of defect alone the magnetization direction. The vertical edge can be recognized by detecting the maximum and the minimum of the gradient value of *Bx* alone the magnetization direction. However, *Bx* is insensitive to the horizontal edge of defects. This mainly because the horizontal edge is along to the magnetization direction. Thus, the magnetic flux line, paralleling to the magnetization direction do not have significant fluctuations around the horizontal edge.

The normal component *Bz* of MFL signal reflects the changing trend of the defect depth in normal direction. Since there is a certain change of depth at the edge of the defect, *Bz* can also be used to recognize the edge contour of defect, too. As shown in Fig.2. (c), *Bz* is also sensitive to the vertical edge of defect, but insensitive to the horizontal edge of defects as the horizontal component *Bx*. For the normal component signal *Bz*, the horizontal edge of defect appears around the peak value of *Bz* along the magnetization direction.

According to the above analysis, *Bx* and *Bz* have the similar edge recognition sensitivity of defect. They are commonly used to detect the opening profile of defect. The horizontal component signal is more often be chosen to deal with the opening profile recognition problem, especially under the 1-D MFL measurement condition. The gradient detection operation of *Bx* is used to realize the recognition of non-horizontal edges of defect. If the edge of defect contains a certain of vertical component, it can be easily detected by *Bx*.

Besides the edge of defect, the angle is another important feature of defect. Right-angle, as the interaction between the horizontal edge and vertical edge of defect, is difficult to be recognized by either *Bx* or *Bz*. However, right-angle is essential for the topological description of the whole defect. Therefore, other signal information need to be introduced to analyze the important right-angle feature.

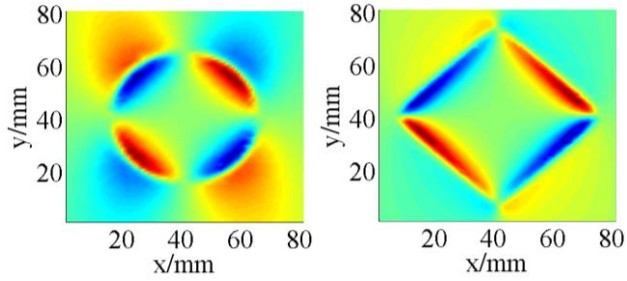

(a) Circular defect (b) Diamond defect

Fig. 4. Vertical component signal image for other features

C. *Characteristics of Vertical MFL Signals*

The vertical component *By* of MFL signal reflects the changing trend of the MFL signal in the vertical direction. As shown in Fig.2. (b), *By* is neither sensitive to the vertical edge of defect nor sensitive to the horizontal edge of defect. This gives a reasonable explain that why the *Bx* or *Bz* is preferred being used to recognized the profile of defect rather than *By* in 1-D MFL measurement system. However, the vertical component signal *By* is sensitive to the right angle of defect. The vertical component *By* located in the right-angle shows a peak or valley tendency feature. This phenomenon shows the right-angle feature of vertical component of MFL signal.

By observing all kinds of right-angles of defect and their corresponding vertical component signals, the signal features for different right-angles can be summarized. Fig.3. (a) gives the all eight kinds of right-angles and Fig.3. (b) shows their corresponding vertical component responses in the *By* signal image.

As can be seen in Fig.3., For different right-angles, their vertical component responses are different. they can be summarized into two categories. One is the peak type, the vertical component signal *By* shows a peak shape and reaches to the maximum at the right-angle point of defect. The peak type corresponds to four kinds of right-angles I, III, V, VII in Fig.3. (a). The other is the valley type, the vertical component signal *By* shows a valley shape and falls to the minimum at the right-angle point of defect. The valley type corresponds to the other four kinds of right-angles II, IV, VI, VIII in Fig.3. (a). Table I gives the detail classification.

Table I shows that every kind of right-angle of defect can be allocated to a feature type according to its characteristic of vertical component response. These right-angle types can be identified by *By*. This property is particular for the vertical component signal rather than the horizontal or normal component signal. Therefore, *By* can be considered to applied to further optimized the opening profile of defect based on its right-angle feature.

III. IDENTIFICATION OF RIGHT-ANGLE TYPE

The right-angle feature is an important and useful feature of defect for the vertical component signal *By*. However, it should be distinguished from other edge features of *By* carefully. Fig.4. shows the vertical component signal images of a circular defect and a diamond defect, separately. It can be seen that, *By* also responses to the arc edge and oblique edge. In order to

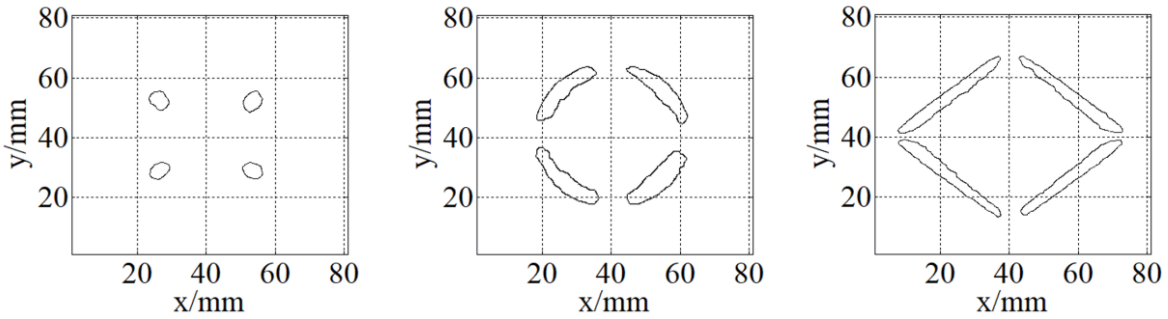

(a) rectangular defect (b) circular defect (c) diamond defect

Fig.5. Detected contours of different defects

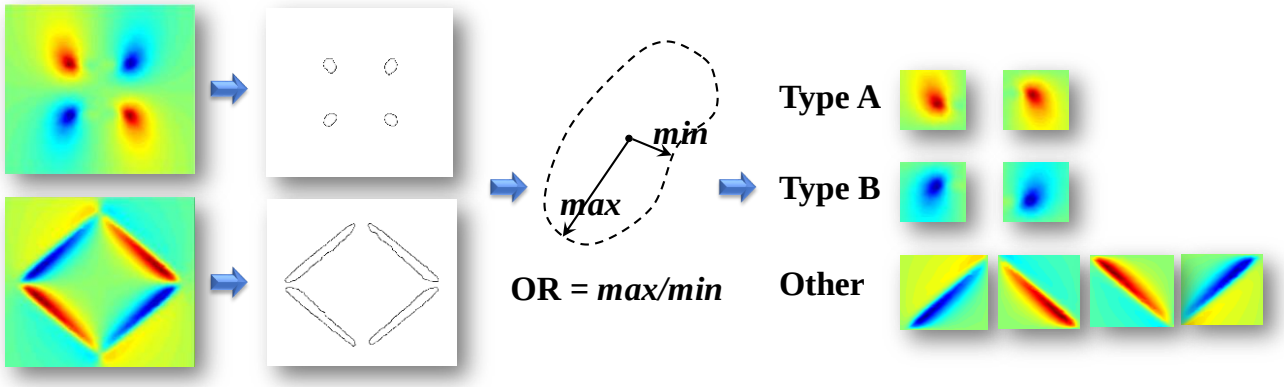

Fig.6. Procedure of the right-angle identification

distinguish the right-angle feature from the different vertical component features, the contour of each vertical component feature is detected and analyzed here. Using the Canny edge detection algorithm [22] to detect the contour of each feature. Fig.5 shows the detected results for the rectangular defect, circular defect and the diamond defect, separately.

It can be seen, only the contour of right-angle feature is approximately a circle. Therefore, an index of out-of-roundness (OR) of contour is defined as follows to identify the right-angle feature. The OR is the ratio of the maximum distance to the minimum distance from the contour to its centroid.

$$\mathrm{OR} = \frac{\max\{\sqrt{(x_i - x_c)^2 + (y_i - y_c)^2}\}}{\min\{\sqrt{(x_j - x_c)^2 + (y_i - y_c)^2}\}} \tag{5}$$

Where, (x_i, y_i), (x_j, y_j) are the position of the pixels in the contour. (x_c, y_c) is the position of the centroid of the contour. $\mathrm{OR} \geq 1$.

Since the OR is introduced to evaluate the roundness of the contour, the procedure of the right-angle identification can be implemented as follows.

1) Select the normalized vertical component of MFL signal area to be identified.

2) Adopt the Canny edge detection algorithm to detect the contours of feature from the signal area.

3) Calculate the position of the centroid $P_c(x_c, y_c)$ of each contour by the following expression.

$$x_c = \frac{\sum_{k=1}^{N} x_k}{N}, \quad y_c = \frac{\sum_{k=1}^{N} y_k}{N} \tag{6}$$

Where, N is the total number of the pixels in the contour.

4) Calculate the OR of each contour by equation (5).

5) Set an appropriate threshold H. Select the contour area of which OR is in the range [1, H] as the right-angle area.

6) Sort the right-angle area into peak type area A_p or valley type area A_v. These simply-connected areas are constrained by the following conditions:

$$\forall P(x, y) \in A_p, \quad B_y(x, y) \geq T_p \tag{7}$$

$$\forall P(x, y) \in A_v, \quad B_y(x, y) \leq T_v \tag{8}$$

Where, By (x, y) is the vertical component of MFL signal strength at the point $P(x, y)$ in the right-angle area. T_p and T_v are the thresholds for the peak type and valley type areas of signal, separately.

7) Obtain the right-angle point $P_{rt}(\hat{x}, \hat{y})$ for each identified area. For the peak type area A_p the right-angle point is the maximum signal strength point in this area. For the valley type area A_v, it's the minimum point.

The above procedure is also summarized in Fig.6 to illustrate the procedure more clearly.

IV. Opening Profile Recognition Method

Since the right-angle type of defect can be detected from the vertical component signal, the certain kind of right-angle can be further identified. Based on the right-angle type identification, an opening profile recognition method is put forward here. Compared with the traditional method based merely on the horizontal or normal component signal, the proposed method

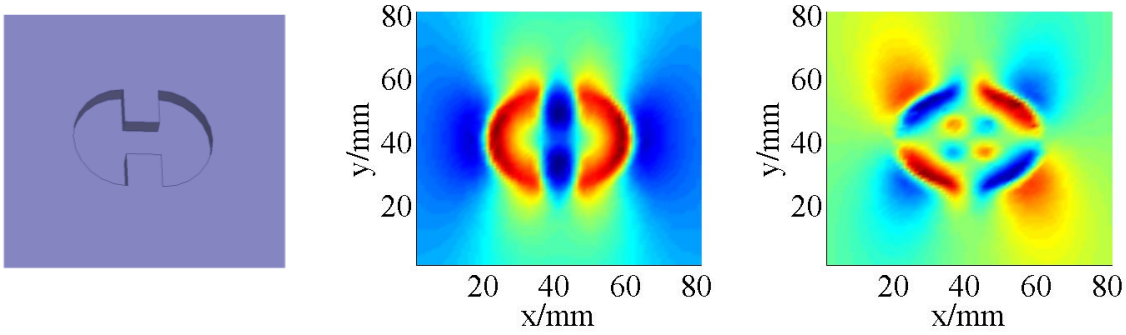

(a) Simulate defect (b) Horizontal component (c) Vertical component

Fig. 7. Simulated defect and MFL signal strength images

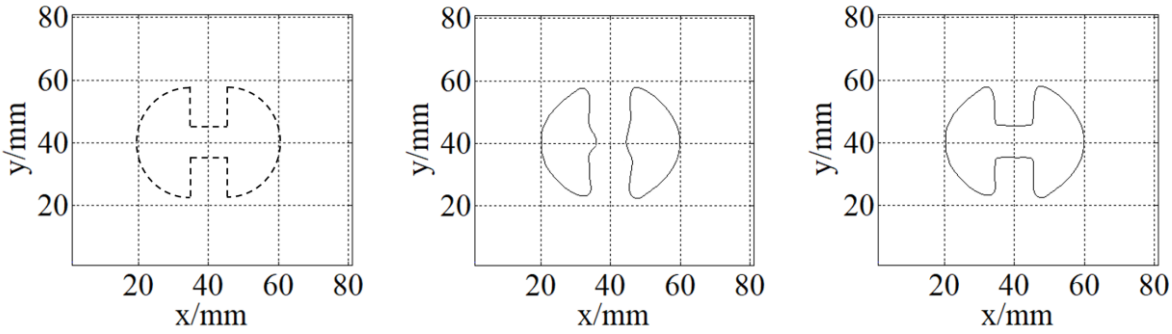

(a) Original profile (b) Initial profile (c) Final profile

Fig. 8. Opening profile recognition of simulation results

TABLE II
ANGLE RANGE OF DIFFERENT KINDS OF RIGHT-ANGLE

Peak Type		Valley Type	
I	[-π/2 , 0]	II	[-π , π/2]
III	[-3π/2 , 0]	IV	[-π , -π/2]
IV	[π/2 , π]	VI	[0 , 3π/2]
VII	[-π/2 , π]	VIII	[0 , π/2]

adds the vertical component signal analysis to further optimize the profile.

The detail of the profile recognition is described in the following steps.

Step I. Conduct the MFL testing for the slab to be detected and obtain the normalized horizontal and vertical component of MFL signal matrix $\boldsymbol{M}_x$ and $\boldsymbol{M}_y$. Select the domain of interest (DOI) where defect exists.

Step II. Recognize the initial opening profile of defect based on *Bx* in DOI. The specific steps are as follows:

1) Adopt the Prewitt operator templates $\boldsymbol{G}_P$ to convolute the horizontal component signal matrix $\boldsymbol{M}_x$ to get the gradient signal matrix $\boldsymbol{P}_x$, which can be expressed as:

$$\boldsymbol{P}_x = \boldsymbol{G}_P * \boldsymbol{M}_x \tag{9}$$

Where, $*$ is the convolution operator.

2) Take the maximum of gradient signal matrix in the direction of the convolution as the edge pixels of defect.

3) Curve fitting of these edge pixels to get the initial opening profile of defect. Adopt the binarization operation to obtain the binary area of defect.

Step III. Optimize the opening profile of defect based on *By*. The specific steps are as follows:

1) Identify the right-angle type from the vertical component signal *By* according the procedure presented in *Section III*.

2) If there is right-angle feature exist, record the right-angle point $P(\hat{x},\hat{y})$. Traverse every edge pixel $P_i(x_i,y_i)$ to calculate the angle θ_i between $P(\hat{x},\hat{y})$ and $P_i(x_i,y_i)$, which can be expressed as:

$$\theta_i = \arctan\frac{y_i-\hat{y}}{x_i-\hat{x}} + (1-\frac{|x_i-\hat{x}|}{\hat{x}-x_i})\cdot\pi$$

Where, $i = 1, 2, \ldots, N$. N is the total number of the edge pixels.

Else, it means the defect exists no right-angle. Skip to step IV directly.

3) Compare the calculated angle θ_i with the angle range of different kinds of right-angle given in Table II. Calculated the probabilities that θ_i fall into the angle range of different kinds of right-angle.

4) Pick the right-angle kind of which angle range corresponding to the maximum probability as the kind of the right-angle. Revise the opening profile according the obtained kind of right-angle.

5) Based on the identified right-angle kind and its position $P(\hat{x},\hat{y})$, revise the binary area of defect.

Step IV. Adopt the Canny edge detection algorithm to recognize the final opening profile from the revised binary area

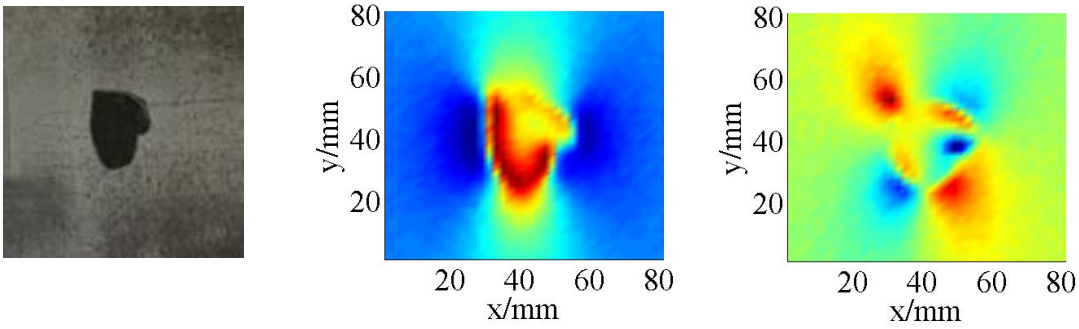

(a) Metal-loss defect (b) Horizontal component (c) Vertical component

Fig. 9. Metal-loss defect and MFL signal strength images

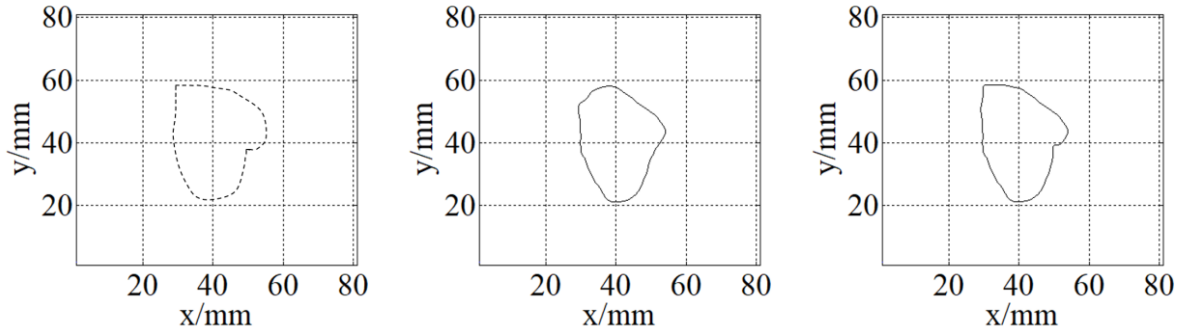

(a) Original profile (b) Initial profile (c) Final profile

Fig. 10. Opening profile recognition of experimental results

of defect.

V. Results And Discussion

In order to verify the proposed opening profile recognition method, both simulation and experimental tests are conducted here.

A. Simulation Results

Using the finite element model established in Fig.1 to simulate the special MFL signal of an arbitrary defect. This defect shown in Fig.7 (a) contains four different kinds of right-angle II, III, VI, VII. The thickness of the steel slab is 12mm. The lift-off value is 2mm. Figs.7 (b) and (c) draw the normalized horizontal and vertical component signal images of the simulated defect, separately.

By detecting the right-angle features of the vertical component of MFL signal, four right-angels can be identified. Adopt the recognition method proposed in *Section IV*. The Opening profile recognition results are shown in Fig.8. Fig.8 (a) is the original opening profile of the simulated defect. Fig.8 (b) is the detected initial opening profile by *Step II*. It can be seen that, for the horizontal component of MFL signal, the right-angle connected area is too narrow to be detected. After the optimize operation in *Step III*, the information of four kinds of right-angle of defect II, III, VI, VII are identified. The final opening profile of defect are shown in Fig.8 (c).

The simulated results show that, recognize the opening profile of defect only by horizontal signal is not always accurate. In some cases, if the narrow connected area is in the horizontal direction, one defect may be recognized as two, which will lead to the estimation failure of defect. Introducing the vertical component signal analysis can detect more critical features of defect and make the recognition result more accurate.

B. Experimental Results

In order to further examine the significance of the vertical component of MFL signal and the performance of the proposed method, this method is applied to the profile recognition of a real metal-loss defect whose MFL signals are obtained by MFL measurement system. During the measurement process, the lift-off value is 2.3mm and the sampling interval is 2mm. The thickness of the steel slab is 10mm. The opening profile of the defect is shown in Fig.9 (a). It contains two different kinds of right-angle I and VI. Figs.9 (b) and (c) draw the measured horizontal and vertical component of MFL signal images of defect, separately.

Fig.10 (a) gives the original opening profile of the metal-loss defect as the reference. Fig.10 (b) presents the initial opening profile by *Step II*. The initial profile is obtained by the horizontal component of MFL signal merely. Conducting the optimize operation in *Step III* and *IV*, two right-angles I and VI are identified. The final opening profile of defect are shown in Fig.10 (c).

Compared with the initial profile and final profile of the defect, the final profile is closer to the original profile and can reflect the right-angle features clearly.

To quantify and compare the accuracy of the different recognized results, the error between the recognized profile and the original profile is defined as follows. The calculated errors for these two tests shown in Table III.

TABLE III
ERRORS OF THE RESULTS

Results	Initial profile	Final profile
Simulate results	0.127	0.077
Experimental results	0.082	0.065

$$e = \frac{S\left[\left(P_R \setminus P_O\right) \cup \left(P_O \setminus P_R\right)\right]}{S\left[P_O\right]} \tag{20}$$

Where, P_R represents the pixel set of recognized profile and its inner points, and P_O represents that of original profile and its inner points. $P_R \setminus P_O$ represents the difference set from $P_R - P_O$. $S[\bullet]$ represents the pixel area surrounded by the corresponding profile.

Both simulation and experimental results show that the vertical component of MFL signal can reveal the important right-angle of defect and examine the validity and accuracy of the proposed opening profile recognition method. It should be noticed that, the proposed method is based on the right-angle feature of vertical component signal to optimize the opening profile of defect. If the defect has no right-angle or approximate right-angle, there is no need to further optimize the profile. Because, for a non-right-angle of defect, it surely contains the vertical component of the edge which the horizontal component signal is sensitive to. Thus, the opening profile of defect can be well recognized from the horizontal component of MFL signal. But for the right-angle of defect, it contains the pure horizontal component edge which the horizontal component signal is insensitive to. So, the right-angle feature of defect is hard to be recognized by merely horizontal component signal. For many workpieces, the right-angle is commonly appeared in the defect due to some man-made destruction factors. So the vertical component signal analysis is necessary and useful for the defective opening profile recognition.

In this paper, only horizontal component signal, rather than normal component signal, is adopted to obtain the initial profile. This is because the horizontal component signal is more commonly used than normal one for the defective profile recognition. Besides, the horizontal and normal component signals has the similar detect effect for the opening profile of defect. Thus, the proposed method can also adopt the normal component signal to obtain the initial opening profile which has the same effect for the final recognition.

VI. Conclusion

This paper analyzes the specific right-angle feature of the vertical component of MFL signal. To distinguish with other features, a certain procedure is given to identify the right-angle type from the vertical component signal. This right-angle feature can be used to optimize the opening profile of defect besides the horizontal or normal component signal. In this paper, an opening profile recognition method which taken the vertical component signal into account is proposed. This method presents a four steps procedure to recognize the opening profile of defect. Not only detect the initial profile from the horizontal component signal, but also optimize the profile by the vertical component signal features. Both the simulation and experimental tests validate the effectiveness and accuracy of the proposed recognition method. Since the right-angle is a commonly feature of defect, the proposed method is necessary and useful for the defective opening profile recognition.

Acknowledgment

This research was supported by the National Natural Science Foundation of China (NSFC) (No. 51677093) and the National Key Scientific Instrument Development Projects (No 2013YQ140505).

References

[1] J. Feng, F. M. Li, S. X. Lu, J. H. Liu and D. Z. Ma, "Injurious or Noninjurious Defect Identification From MFL Images in Pipeline Inspection Using Convolutional Neural Network," *IEEE Trans. Instrum. Meas.*, vol. 66, no. 7 pp. 1883–1892, Jul. 2017.

[2] A. V. Joshi, L. Udpa, S. S. Udpa and A. Tamburrino, "Adaptive wavelets for characterizing magnetic flux leakage signals from pipeline inspection," *IEEE Trans. Magn.*, vol. 42, no. 10, pp. 3168–3170, Jun. 2006.

[3] Y.Melikhov, S. J. Lee, D. C. Jiles and R. Lopez, "Analytical approach for fast computation of magnetic flux leakage due to surface defects". *2005 IEEE International Magnetics Conference (INTERMAG)*, vol. 22, no. 1, pp. 1165-1166, Jul. 2005.

[4] J. H. Liu, M. R. Fu, F. L. Liu, J. Feng and K. Q. Cui, "Window Feature-Based Two-Stage Defect Identification Using Magnetic Flux Leakage Measurements," *IEEE Trans. Instrum. Meas.*, vol. 67, no. 1 pp. 12–23, Jan. 2018.

[5] N. Kasai, K. Sekine and H. Maruyama, "Non-Destructive Evaluation Method for Far-Side Corrosion Type Flaws in Oil Storage Tank Bottom Floors Using the Magnetic Flux Leakage Technique," *J. Jpn. Petrol Inst.*, vol. 46, no. 2, pp. 126-132, Aug. 2003.

[6] R. H. Priewald, C. Magele, P. D. Ledger, N. R. Pearson and J. S. D. Mason, "Fast Magnetic Flux Leakage Signal Inversion for The Reconstruction of Arbitrary Defect Profiles in Steel Using Finite Elements", *IEEE Trans. Magn.*, vol. 49, no. 1, pp. 506-516, Jan. 2013.

[7] J. J. Chen, S. L. Huang and W. Zhao, "Three-Dimensional Defect Reconstruction From Magnetic Flux Leakage Signals in Pipeline Inspection Based on A Dynamic Taboo Search Procedure." *Insight.*, vol. 56, no. 10, pp. 535-540, Oct. 2014.

[8] J. Feng, F. M. LI, S. X. Lu and J. H. Liu, "Fast Reconstruction of Defect Profiles from Magnetic Flux Leakage Measurements Using A RBFNN Based Error Adjustment Methodology," *IET Sci. Meas. Technol.*, vol. 11, no. 3, pp. 262-269, May. 2017.

[9] B. Wijerathna, S. Kodagoda, J. V. Miro and G. Dissanayake, "Iterative Coarse to Fine Approach for Interpretation of Defect Profiles Using MFL Measurements," presented at the IEEE 10th Conference on Industrial Electronics and Applications (ICIEA), Auckland, New Zealand, Nov. 1099–1104, 2015.

[10] A. V. Joshi, L. Udpa, S. S. Udpa and A. Tamburrino, "Adaptive Wavelets for Characterizing Magnetic Flux Leakage Signals from Pipeline Inspection,". *IEEE Trans. Magn.*, vol. 42, no. 10, pp. 3168-3170, Jun. 2006.

[11] S. M. Dutta, F. H. Ghorbel and R. K. Stanley, "Simulation and Analysis of 3-D Magnetic Flux Leakage," *IEEE Trans. Magn.*, vol. 45, no. 4, pp. 1966-1972, Apr. 2009.

[12] M. Ravan, R. K. Amineh, S. Koziel, N. K. Nikolova and J. P. Reilly, "Sizing of 3-D Arbitrary Defects Using Magnetic Flux Leakage Measurements," *IEEE Trans. Magn.*, vol. 46, no. 4, pp. 1024-1033, Dec. 2010.

[13] R. K. Amineh, N. K. Nikolova, J. P. Reilly and J. R. Hare, "Characterization of Surface-Breaking Cracks Using One Tangential Component of Magnetic Leakage Field Measurements," *IEEE Trans. Magn..*, vol. 44, no. 4, pp. 516-524, Apr. 2008

[14] F. M. Li, J. Feng, H. G. Zhang, J. H. Liu, S. X. Lu and D. Z. Ma, "Quick Reconstruction of Arbitrary Pipeline Defect Profiles From MFL Measurements Employing Modified Harmony Search Algorithm," *IEEE Trans. Instrum. Meas.*, Early Access, issue. 99, pp. 1–14, Mar. 2018.

[15] R. H. Priewald, C. Magele, P. D. Ledger, N. R. Pearson and J. S. D. Mason, "Fast Magnetic flux leakage signal inversion for the reconstruction of arbitrary defect profiles in steel using finite elements", *IEEE Trans. Magn.*, vol. 49, no. 1, pp. 506-516, Jan. 2013.
[16] S. L. Huang, L. S. Peng, Q. Wang, S. Wang and W. Zhao, "A Defect Opening Profile Estimation Method Based on the Right-Angle Characteristic of Vertical Component of MFL Signal," *Proceedings of 2018 Conference on Precision Electromagnetic Measurements*, pp. 1–2, 2018.
[17] H. Schempf, E. Mutschler, A. Gavaert, G. Skoptsov and W. Crowley, "Visual and Nondestructive Evaluation Inspection of Live Gas Mains Using the Explorer™ Family of Pipe Robots," *Journal of Field Robotics*, vol. 27, no. 3, pp. 217-249, Jan. 2010.
[18] E. B. Johnston, "Gas Operations News - Internal Inspection Technologies," Gas Technology Institute, Des Plaines, Illinois, USA, Tech. Rep. vol. 10, no. 1, May. 2013.
[19] Y. Shi, C. Zhang, R. Li, M. L. Cai and G. W. Jia, "Theory and Application of Magnetic Flux Leakage Pipeline Detection," *Sensors*, vol. 15, no. 12, pp. 31036-31055, Dec. 2015.
[20] G. S. Park and E. S. Park, "Improvement of the sensor system in magnetic flux leakage-type nondestructive testing (NDT)," *IEEE Trans. Magn.*, vol. 38, no. 2, pp. 1277–1280, Mar. 2002.
[21] G. S. Park, S. Y. Hahn, K. S. Lee, and H. K. Jung, "Implementation of hysteresis characteristics using Preisach model with M-B variables," *IEEE Trans. Magn.*, vol. 29, pp. 1542–1545, Mar. 1993.
[22] J. Canny. "A computational approach to edge detection", *IEEE Transactions on Pattern Analysis and Machine Intelligence*, vol. 8, no. 6, pp. 679–698, Nov. 1986.

Songling Huang received the bachelor's degree in automatic control engineering from Southeast University, Nanjing, China, in 1991, and the Ph.D. degree in nuclear application technology from Tsinghua University, Beijing, China, in 2001.

He is currently a Professor within the Department of Electrical Engineering, Tsinghua University. His research interests include nondestructive evaluation and instrument techniques.

Lisha Peng received the bachelor's degree from Wuhan University, Hubei, China, in 2014. She is currently pursuing the Ph.D. degree within the Department of Electrical Engineering, Tsinghua University. Her current research interests include magnetic flux leakage (MFL) measurement and defect estimation.

Qing Wang received the B.Eng. in electronic instrument and measurement technique from Beihang University, Beijing, China, in 1995, the M.Sc. degree in advanced manufacturing and materials from the University of Hull, Hull, U.K., in 1998, and the Ph.D. degree in manufacturing management from De Montfort University, Leicester, U.K., in 2001.

She is currently an Associate Professor in the School of Engineering and Computing Sciences, Durham University, Durham, U.K. Her research interests include electronic instruments and measurement, computer simulation, and advanced manufacturing technology.

Shen Wang received the bachelor's and Ph.D. degrees in electrical engineering from Tsinghua University, Beijing, China, in 2002 and 2008, respectively.

He is currently a Research Assistant within the Department of Electrical Engineering, Tsinghua University. His research interests include nondestructive testing and evaluation, and virtual instrumentation.

Wei Zhao received the bachelor's degree in electrical engineering from Tsinghua University, Beijing, China, in 1982, and the Ph.D. degree from the Moscow Power Engineering Institute Technical University, Moscow, Russia, in 1991.

He is currently a Professor within the Department of Electrical Engineering, Tsinghua University. His research interests include modern electromagnetic measurement and instrument techniques.